5. Bearing internal load distribution and displacement

5.1 Bearing internal load distribution

This section will begin by examing the effect of a radial load F_r and an axial load F_a applied on a single-row bearing with a contact angle α (angular contact ball bearings, tapered roller bearings, etc.). The ratio of F_a to F_r determines the range of the loading area when just a portion of the raceway sustains the load, or when the entire raceway circumference sustains the load.

The size of the loading area is called the load factor ε. When only a part of the outer circumference bears the load, ε is the ratio between the projected length of the loading area and the raceway diameter. For this example, we use $\varepsilon \leqq 1$. (Refer to **Fig. 1**).

When the entire raceway circumference is subjected to a load, the calculation becomes,

$$\varepsilon = \frac{\delta_{max}}{\delta_{max} - \delta_{min}} \geqq 1$$

where, δ_{max}: Elastic deformation of a rolling element under maximum load

δ_{min}: Elastic deformation of a rolling element under minimum load

The load $Q(\psi)$ on any random rolling element is proportional to the amount of elastic deformation $\delta(\psi)$ of the contact surface raised to the t power. Therefore, it follows that when $\psi=0$ (with maximum rolling element load of Q_{max} and maximum elastic deformation of δ_{max}),

$$\frac{Q(\psi)}{Q_{max}} = \left(\frac{\delta(\psi)}{\delta_{max}}\right)^t \quad \cdots\cdots (1)$$

t=1.5 (point contact), t=1.1 (line contact)

The relations between the maximum rolling element load Q_{max}, radial load F_r, and axial load F_a are as follows:

$$F_r = J_r Z Q_{max} \cos\alpha \quad \cdots\cdots (2)$$

$$F_a = J_a Z Q_{max} \sin\alpha \quad \cdots\cdots (3)$$

where Z is the number of rolling elements, and J_r and J_a are coefficients for point and line contact derived from **Equation** (1). The values for J_r and J_a with corresponding ε values are given in **Table 1**. When ε=0.5, (when half of the raceway circumference is subjected to a load), the relationship between F_a and F_r becomes,

$F_a = 1.216\, F_r \tan\alpha$ ····· (point contact)

$F_a = 1.260\, F_r \tan\alpha$ ····· (line contact)

The basic load rating of radial bearings becomes significant under these conditions.

Assuming the internal clearance in a bearing Δ=0, ε=0.5 and using a value for J_r taken from **Table 1**, **Equation** (2) becomes,

$$Q_{max} = 4.37\frac{F_r}{Z\cos\alpha} \quad \text{point contact} \quad \cdots\cdots (4)$$

$$Q_{max} = 4.08\frac{F_r}{Z\cos\alpha} \quad \text{line contact} \quad \cdots\cdots (5)$$

With a pure axial load, F_r=0, $\varepsilon=\infty$, J_a=1, and **Equation** (3) becomes;

$$Q = Q_{max} = \frac{F_a}{Z\sin\alpha} \quad \cdots\cdots (6)$$

(In this case, the rolling elements all share the load equally.)

For a single-row deep groove ball bearing with zero clearance that is subjected to a pure radial load, the equation becomes;

$$Q_{max} = 4.37\frac{F_r}{Z} \quad \cdots\cdots (7)$$

For a bearing with a clearance Δ>0 subjected to a radial load and with ε<0.5, the maximum rolling element load will be greater than that given by **Equation** (7). Also, if the outer ring is mounted with a clearance fit, the outer ring deformation will reduce the load range. **Equation** (8) is a more practical relation than **Equation** (7), since bearings usually operate with some internal clearance.

$$Q_{max} = 5\frac{F_r}{Z} \quad \cdots\cdots (8)$$

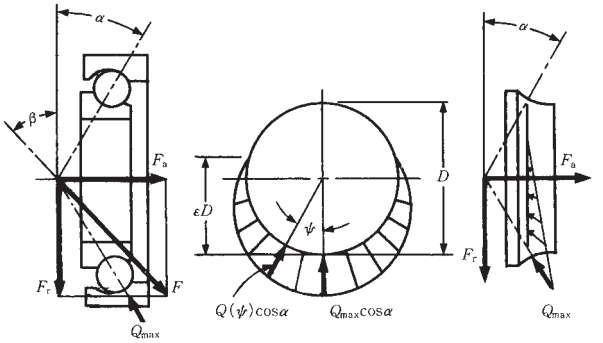

Fig. 1

Table 1 Values for J_r and J_a in single-row bearings

ε	Point contact			Line contact		
	$\frac{F_r\tan\alpha}{F_a}$	J_r	J_a	$\frac{F_r\tan\alpha}{F_a}$	J_r	J_a
0	1	0	0	1	0	0
0.1	0.9663	0.1156	0.1196	0.9613	0.1268	0.1319
0.2	0.9318	0.1590	0.1707	0.9215	0.1737	0.1885
0.3	0.8964	0.1892	0.2110	0.8805	0.2055	0.2334
0.4	0.8601	0.2117	0.2462	0.8380	0.2286	0.2728
0.5	0.8225	0.2288	0.2782	0.7939	0.2453	0.3090
0.6	0.7835	0.2416	0.3084	0.7480	0.2568	0.3433
0.7	0.7427	0.2505	0.3374	0.6999	0.2636	0.3766
0.8	0.6995	0.2559	0.3658	0.6486	0.2658	0.4098
0.9	0.6529	0.2576	0.3945	0.5920	0.2628	0.4439
1.0	0.6000	0.2546	0.4244	0.5238	0.2523	0.4817
1.25	0.4338	0.2289	0.5044	0.3598	0.2078	0.5775
1.67	0.3088	0.1871	0.6060	0.2340	0.1589	0.6790
2.5	0.1850	0.1339	0.7240	0.1372	0.1075	0.7837
5	0.0831	0.0711	0.8558	0.0611	0.0544	0.8909
∞	0	0	1	0	0	1

5.2 Radial clearance and load factor for radial ball bearings

The load distribution will differ if there is some radial clearance. If any load acts on a bearing, in order for the inner and outer rings to maintain parallel rotation, the inner and outer rings must move relative to each other out of their original unloaded position. Movement in the axial direction is symbolized by δ_a and that in the radial direction by δ_r. With a radial clearance Δ_r and a contact angle α, as shown in **Fig. 1**, the total elastic deformation $\delta(\psi)$ of a rolling element at the angle ψ is given by **Equation** (1).

$$\delta(\psi)=\delta_r\cos\psi\cos\alpha+\delta_a\sin\alpha-\frac{\Delta_r}{2}\cos\alpha \quad \cdots\cdots (1)$$

The maximum displacement δ_{max} with $\psi=0$ is given,

$$\delta_{max}=\delta_r\cos\psi+\delta_a\sin\alpha-\frac{\Delta_r}{2}\cos\alpha \quad \cdots\cdots (2)$$

Combining these two equations,

$$\delta(\psi)=\delta_{max}\left\{1-\frac{1}{2\varepsilon}(1-\cos\psi)\right\} \quad \cdots\cdots (3)$$

and,

$$\varepsilon=\frac{\delta_{max}}{2\delta_r\cos\alpha}=\frac{1}{2}\left\{1+\frac{\delta_a}{\delta_r}\tan\alpha-\frac{\Delta_r}{2\delta_r}\right\} \quad \cdots\cdots (4)$$

When there is no relative movement in the axial direction, ($\delta_a=0$), **Equations** (2) and (4) become,

$$\delta_{max}=\left(\delta_r-\frac{\Delta_r}{2}\right)\cos\alpha \quad \cdots\cdots (2)'$$

$$\varepsilon=\frac{1}{2}\left(1-\frac{\Delta_r}{2\delta_r}\right) \quad \cdots\cdots (4)'$$

$$\therefore\ \delta_{max}=\frac{\varepsilon}{1-\varepsilon}\Delta_r\cos\alpha \quad \cdots\cdots (5)$$

From the Hertz equation,

$$\delta_{max}=c\frac{Q_{max}^{2/3}}{D_w^{1/3}} \quad \cdots\cdots (6)$$

The maximum rolling element load Q_{max} is given by,

$$Q_{max}=\frac{F_r}{J_rZ\cos\alpha} \quad \cdots\cdots (7)$$

Combining **Equations** (5), (6), and (7) yields **Equation** (8) which shows the relation among radial clearance, radial load, and load factor.

$$\Delta_r=\left(\frac{1-2\varepsilon}{\varepsilon}J_r^{-2/3}\right)c\left(\frac{F_r}{Z}\right)^{2/3}D_w^{-1/3}\cos^{-5/3}\alpha \quad \cdots\cdots (8)$$

where, Δ_r: Radial clearance (mm)
ε: Load factor
J_r: Radial integral (Page 111, Table 1)
c: Hertz elasticity coefficient
F_r: Radial load (N), {kgf}
Z: Number of balls
D_w: Ball diameter (mm)
α: Contact angle (°)

Values obtained using **Equation** (8) for a 6208 single-row radial ball bearing are plotted in **Fig. 2**.

As an example of how to use this graph, assume a radial clearance of 20 μm and $F_r=C_r/10=2\ 910$ N {297 kgf}. The load factor ε is found to be 0.36 from **Fig. 2** and $J_r=0.203$ (Page 111, **Table 1**). The maximum rolling element load Q_{max} can then be calculated as follows,

$$Q_{max}=\frac{F_r}{J_rZ\cos\alpha}=\frac{2\ 910}{0.203\times9}=1\ 590\text{N}\ \{163\text{kgf}\}$$

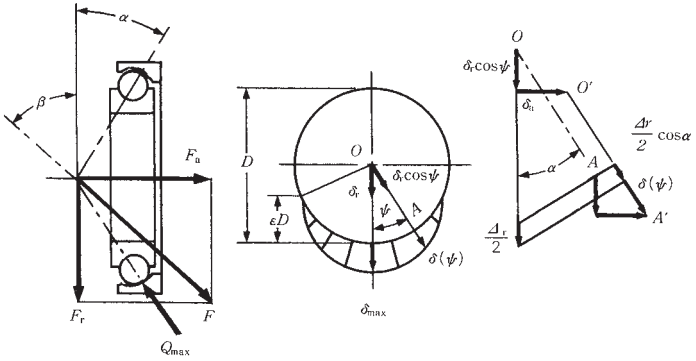

Fig. 1

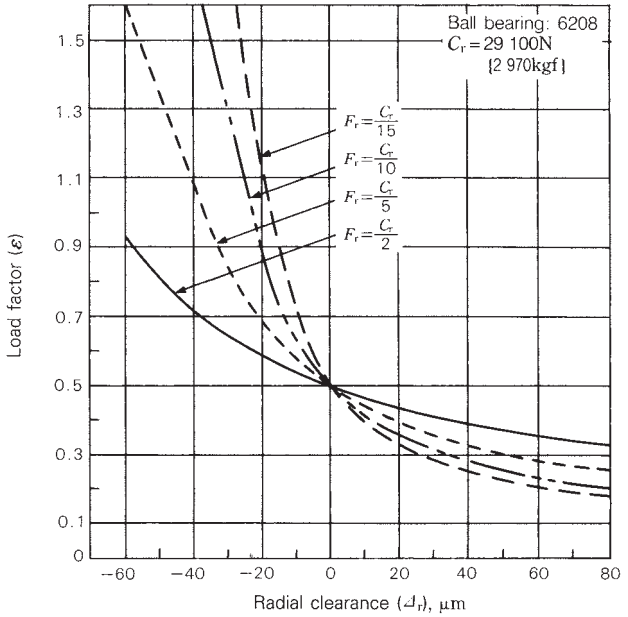

Fig. 2

5.3 Radial clearance and maximum rolling element load

If we consider an example where a deep groove ball bearing is subjected to a radial load and the radial clearance Δ_r is 0, then the load factor ε will be 0.5. When $\Delta_r>0$ (where there is a clearance), $\varepsilon<0.5$; when $\Delta_r<0$, $\varepsilon>0.5$. (See Fig. 1).

Fig. 2 in section 5.2 shows how the load factor change due to clearance decreases with increasing radial load.

When the relationship between radial clearance and load factor is determined, it can be used to establish the relationship between radial clearance and bearing life, and between radial clearance and maximum rolling element load.

The maximum rolling element load is calculated using Equation (1).

$$Q_{max}=\frac{F_r}{J_r Z\cos\alpha} \quad \cdots\cdots (1)$$

where, F_r: Radial load (N), {kgf}
J_r: Radial integral
Z: Number of balls
α: Contact angle (°)

J_r is dependent on the value of ε (Page 111, Table 1), and ε is determined, as explained in Section 5.2, from the radial load and radial clearance.

Fig. 2 shows the relationship between the radial clearance and maximum rolling element load for a 6208 deep groove ball bearing. As can be seen from Fig. 2, the maximum rolling element load increases with increasing radial clearance or reduction in the loaded range. When the radial clearance falls slightly below zero, the loaded range grows widely resulting in minimum in the maximum rolling element load. However, as the compression load on all rolling elements is increased when the clearance is further reduced, the maximum rolling element load begins to increase sharply.

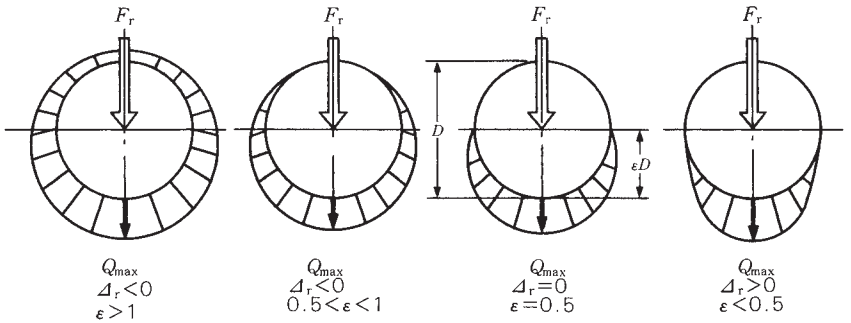

Fig. 1 Radial clearance and load distribution

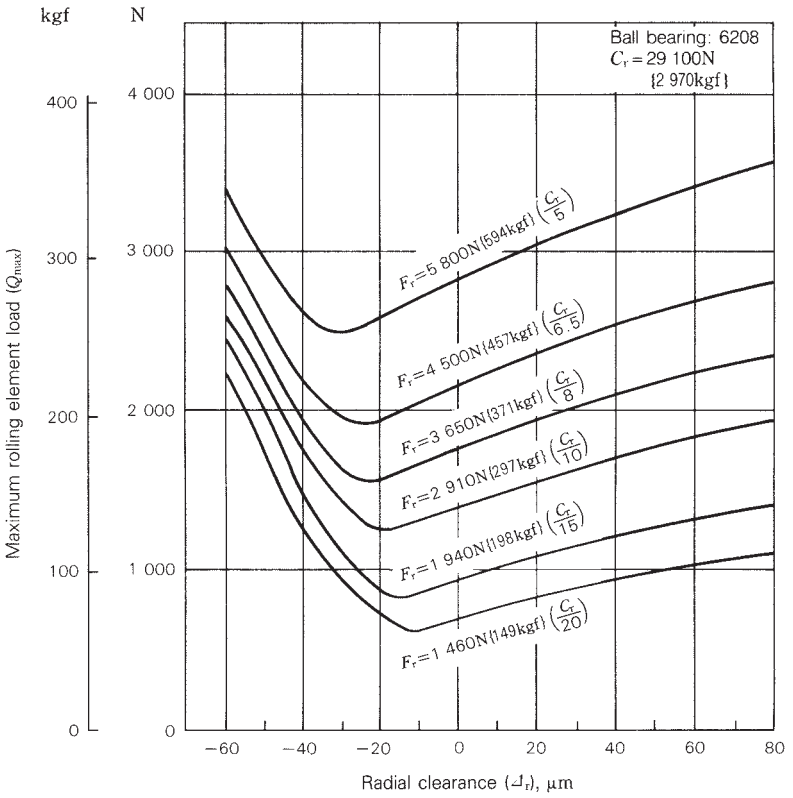

Fig. 2 Radial clearance and maximum rolling element load

5.4 Contact surface pressure and contact ellipse of ball bearings under pure radial loads

Details about the contact between a rolling element and raceway is a classic exercise in the Hertz theory and one where theory and practice have proven to agree well. It also forms the basis for theories on ball bearing life and friction.

Generally, the contact conditions between the inner ring raceway and ball is more severe than those between the outer ring raceway and ball. Moreover, when checking the running trace (rolling contact trace), it is much easier to observe the inner ring raceway than the outer ring raceway. Therefore, we explain the relation of contact ellipse width and load between an inner ring raceway and a ball in a deep groove ball bearing. With no applied load, the ball and inner ring raceway meet at a point. When a load is applied to the bearing, however, elastic deformation is caused and the contact area assumes an elliptical shape as shown in Fig. 1.

When a ball bearing is subjected to a load, the resulting maximum contact surface pressure on the elliptical area of contact between a ball and a bearing raceway is P_{max}. The major axis of the ellipse is represented by $2a$ and the minor axis by $2b$. The following relationships were derived from the Hertz equation.

$$P_{max}=\frac{1.5}{\pi}\left\{\frac{3}{E}\left(1-\frac{1}{m^2}\right)\right\}^{-2/3}\frac{1}{\mu\nu}(\Sigma\rho)^{2/3}Q^{1/3}$$

$$=\frac{A_1}{\mu\nu}(\Sigma\rho)^{2/3}Q^{1/3}$$

(MPa), {kgf/mm^2} ..... (1)

where, Constant A_1: 858 for (N-unit), 187 for {kgf-unit}

$$2a=\mu\left\{\frac{24\left(1-\frac{1}{m^2}\right)Q}{E\Sigma\rho}\right\}^{1/3}$$

$$=A_2\mu\left(\frac{Q}{\Sigma\rho}\right)^{1/3}\quad(\text{mm})\ \cdots\cdots (2)$$

where, Constant A_2: 0.0472 for (N-unit), 0.101 for {kgf-unit}

$$2b=\nu\left\{\frac{24\left(1-\frac{1}{m^2}\right)Q}{E\Sigma\rho}\right\}^{1/3}$$

$$=A_2\nu\left(\frac{Q}{\Sigma\rho}\right)^{1/3}\quad(\text{mm})\ \cdots\cdots (3)$$

where, E: Young's modulus (Steel: E=208 000 MPa {21 200 kgf/mm^2})
m: Poisson's number (Steel: 10/3)
Q: Rolling element (ball) load (N), {kgf}
$\Sigma\rho$: Total major curvature

For radial ball bearing,

$$\Sigma\rho=\frac{1}{D_w}\left(4-\frac{1}{f}\pm\frac{2\gamma}{1\mp\gamma}\right)\ \cdots\cdots (4)$$

Symbol of ±: The upper is for inner ring.
The lower is for outer ring.

D_w: Ball diameter (mm)
f: Ratio of groove radius to ball diameter
γ: $D_w\cos\alpha/D_{pw}$
D_{pw}: Ball pitch diameter (mm)
α: Contact angle (°)

μ and ν are shown in Fig. 2 based on $\cos\tau$ in Equation (5).

$$\cos\tau=\frac{\frac{1}{f}\pm\frac{2\gamma}{1\mp\gamma}}{4-\frac{1}{f}\pm\frac{2\gamma}{1\mp\gamma}}\ \cdots\cdots (5)$$

Symbol of ±: The upper is for the inner ring.
The lower is for the outer ring.

If the maximum rolling element load of the ball bearing under the radial load F_r is Q_{max} and the number of balls is Z, an approximate relation between them is shown in Equation (6).

$$Q_{max}=5\frac{F_r}{Z}\ \cdots\cdots (6)$$

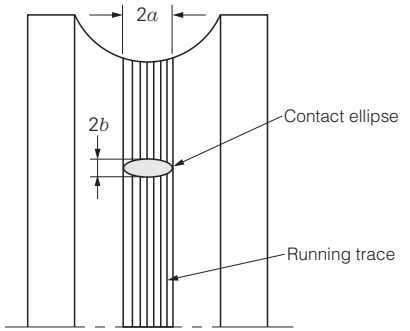

Fig. 1 Inner ring raceway running trace (Rolling contact trace)

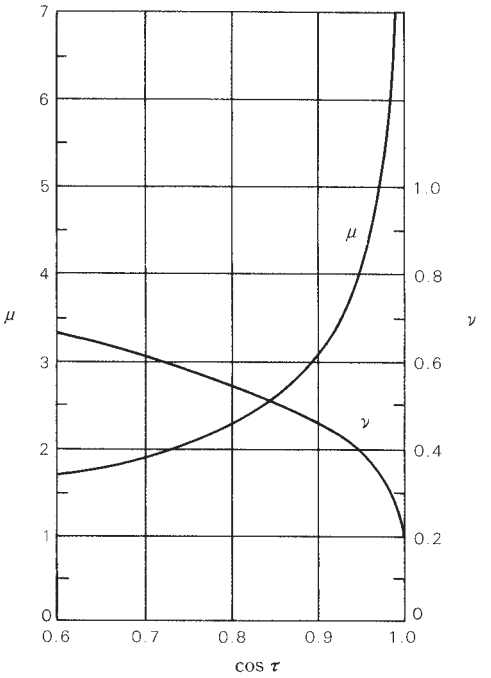

Fig. 2 μ and ν values against $\cos\tau$

Therefore, Equations (1), (2), and (3) can be changed into the following equations by substituting Equations (4) and (6).

$$\left.\begin{aligned} P_{max} &= K_1 \cdot F_r^{1/3} \quad \text{(MPa)} \\ &= 0.218 K_1 \cdot F_r^{1/3} \quad \{\text{kgf/mm}^2\} \end{aligned}\right\} \cdots\cdots\cdots\cdots (7)$$

$$\left.\begin{aligned} 2a &= K_2 \cdot F_r^{1/3} \quad \text{(N)} \\ &= 2.14 K_2 \cdot F_r^{1/3} \quad \{\text{kgf}\} \end{aligned}\right\} \text{(mm)} \cdots\cdots\cdots\cdots (8)$$

$$\left.\begin{aligned} 2b &= K_3 \cdot F_r^{1/3} \quad \text{(N)} \\ &= 2.14 K_3 \cdot F_r^{1/3} \quad \{\text{kgf}\} \end{aligned}\right\} \text{(mm)} \cdots\cdots\cdots\cdots (9)$$

Table 1 gives values for the constants K_1, K_2, and K_3 for different bearing numbers.

Generally, the ball bearing raceway has a running trace caused by the balls whose width is equivalent to $2a$. We can estimate the applied load by referring to the trace on the raceway. Therefore, we can judge whether or not any abnormal load was sustained by the bearing which was beyond what the bearing was originally designed to carry.

Example

The pure radial load, F_r=3 500 N (10% of basic dynamic load rating), is applied to a deep groove ball bearing, 6210. Calculate the maximum surface pressure, P_{max}, and contact widths of the ball and inner ring raceway, $2a$ and $2b$.

Using the figures of K_1 ~ K_3 in Table 1, the following values can be obtained.

$P_{max} = K_1 \cdot F_r^{1/3} = 143 \times 3\ 500^{1/3} = 2\ 170$ (MPa)
$2a = K_2 \cdot F_r^{1/3} = 0.258 \times 3\ 500^{1/3} = 3.92$ (mm)
$2b = K_3 \cdot F_r^{1/3} = 0.026 \times 3\ 500^{1/3} = 0.39$ (mm)

Table 1 Values of constants, K_1, K_2, and K_3, for deep groove ball bearings

Bearing bore No.	Bearing series 60			Bearing series 62			Bearing series 63		
	K_1	K_2	K_3	K_1	K_2	K_3	K_1	K_2	K_3
00	324	0.215	0.020	303	0.205	0.019	215	0.404	0.018
01	305	0.205	0.019	226	0.352	0.017	200	0.423	0.019
02	287	0.196	0.019	211	0.336	0.017	184	0.401	0.019
03	274	0.189	0.018	193	0.356	0.017	171	0.415	0.019
04	191	0.332	0.017	172	0.382	0.018	161	0.431	0.020
05	181	0.320	0.016	162	0.367	0.018	142	0.426	0.020
06	160	0.326	0.017	143	0.395	0.019	129	0.450	0.021
07	148	0.342	0.017	128	0.420	0.020	118	0.474	0.021
08	182	0.205	0.021	157	0.262	0.026	112	0.469	0.023
09	166	0.206	0.021	150	0.252	0.025	129	0.308	0.030
10	161	0.201	0.021	143	0.258	0.026	122	0.318	0.031
11	148	0.219	0.023	133	0.269	0.027	116	0.327	0.032
12	144	0.214	0.022	124	0.275	0.028	110	0.336	0.032
13	140	0.209	0.022	120	0.280	0.028	105	0.344	0.033
14	130	0.224	0.023	116	0.284	0.029	100	0.352	0.034
15	127	0.219	0.023	112	0.275	0.028	96.5	0.356	0.035
16	120	0.235	0.024	109	0.293	0.030	92.8	0.364	0.035
17	117	0.229	0.024	104	0.302	0.031	89.4	0.371	0.036
18	111	0.244	0.025	98.7	0.310	0.031	86.3	0.377	0.037
19	108	0.238	0.025	94.3	0.318	0.032	83.4	0.384	0.037
20	108	0.238	0.025	90.3	0.325	0.033	78.6	0.394	0.038
21	102	0.243	0.026	87.2	0.329	0.033	76.7	0.400	0.039
22	98.2	0.268	0.028	83.9	0.336	0.034	72.7	0.412	0.040
24	95.3	0.261	0.027	80.7	0.343	0.035	72.0	0.411	0.040
26	88.1	0.263	0.028	77.8	0.349	0.035	68.5	0.422	0.041
28	85.9	0.257	0.027	77.2	0.348	0.036	65.5	0.431	0.042
30	81.8	0.264	0.028	74.3	0.337	0.035	62.5	0.414	0.041

5.5 Contact surface pressure and contact area under pure radial load (roller bearings)

The following equations, Equations 1 and 2, which were derived from the Hertz equation, give the contact surface pressure P_{max} between two axially-parallel cylinders and the contact area width $2b$ (Fig. 1).

$$P_{max}=\sqrt{\frac{E\cdot\Sigma\rho\cdot Q}{2\pi\left(1-\frac{1}{m^2}\right)L_{we}}}=A_1\sqrt{\frac{\Sigma\rho\cdot Q}{L_w}}$$

(MPa) {kgf/mm^2} ..... (1)

where, constant A_1: 191 ..... (N-unit)
: 60.9 ..... {kgf-unit}

$$2b=\sqrt{\frac{32\left(1-\frac{1}{m^2}\right)Q}{\pi\cdot E\cdot\Sigma\rho\cdot L_w}}=A_2\sqrt{\frac{Q}{\Sigma\rho\cdot L_w}}$$

(mm) ..... (2)

where, constant A_2: 0.00668 ..... (N-unit)
: 0.0209 ..... {kgf-unit}

where, E: Young's modulus (Steel: E=208 000 MPa {21 200 kgf/mm^2})
m: Poisson's number (for steel, m=10/3)
$\Sigma\rho$: Composite curvature for both cylinders
$\Sigma\rho=\rho_{\mathrm{II}}+\rho_{\mathrm{III}}$ (mm^{-1})
ρ_{II}: Curvature, cylinier I (roller)
$\rho_{\mathrm{II}}=1/D_w/2=2/D_w$ (mm^{-1})
ρ_{III}: Curvature, cylinier II (raceway)
$\rho_{\mathrm{III}}=1/D_i/2=2/D_i$ (mm^{-1}) for inner ring raceway
$\rho_{\mathrm{III}}=-1/D_e/2=-2/D_e$ (mm^{-1}) for outer ring raceway
Q: Normal load on cylinders (N), {kgf}
L_{we}: Effective contact length of cylinders (mm)

When a radial load F_r is applied on a radial roller bearing, the maximum rolling element load Q_{max} for practical use is given by Equation (3).

$$Q_{max}=\frac{4.6\,F_r}{i\,Z\cos\alpha}\quad\text{(N), \{kgf\}}\ \cdots\cdots\ (3)$$

where, i: Number of roller rows
Z: Number of rollers per row
α: Contact angle (°)

The contact surface pressure P_{max} and contact width $2b$ of raceway and roller which sustains the largest load are given by Equations (4) and (5).

$$\left.\begin{aligned}P_{max}&=K_1\sqrt{F_r}&&\text{(MPa)}\\&=0.319K_1\sqrt{F_r}&&\{\text{kgf/mm}^2\}\end{aligned}\right\}\ \cdots\cdots\ (4)$$

$$\left.\begin{aligned}2b&=K_2\sqrt{F_r}&&\text{(N)}\\&=3.13K_2\sqrt{F_r}&&\{\text{kgf}\}\end{aligned}\right\}\ \cdots\cdots\ (5)$$

The constant K_1 and K_2 of cylindrical roller bearings and tapered roller bearings are listed in Tables 1 to 6 according to the bearing numbers. K_{1i} and K_{2i} are the constants for the contact of roller and inner ring raceway, and K_{1e} and K_{2e} are the constants for the contact of roller and outer ring raceway.

Example

A pure radial load, F_r=4 800 N (10% of basic dynamic load rating), is applied to the cylindrical roller bearing, NU210. Calculate the maximum surface pressure, P_{max}, and contact widths of the roller and raceway, $2b$.

Using the figures of K_{1i}, K_{1e} K_{2i}, and K_{2e} in Table 1, the following values can be obtained.

Contact of roller and inner ring raceway:
$P_{max}=K_{1i}\sqrt{F_r}=17.0\times\sqrt{4\ 800}=1\ 180$ (MPa)
$2b=K_{2i}\sqrt{F_r}=2.55\times10^{-3}\times\sqrt{4\ 800}=0.18$ (mm)

Contact of roller and outer ring raceway:
$P_{max}=K_{1e}\sqrt{F_r}=14.7\times\sqrt{4\ 800}=1\ 020$ (MPa)
$2b=K_{2e}\sqrt{F_r}=2.95\times10^{-3}\times\sqrt{4\ 800}=0.20$ (mm)

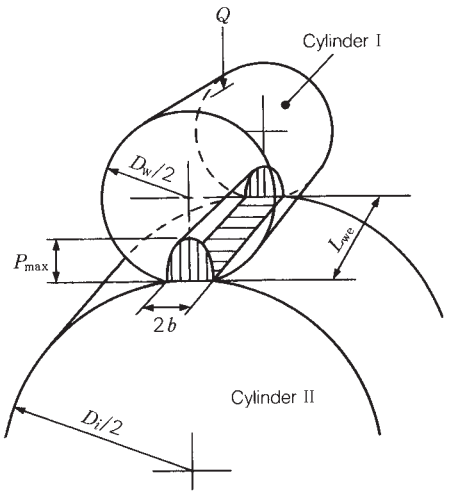

Fig. 1 Contact surface pressure P_{max} and contact width $2b$

Table 1 Constants, K_{1i}, K_{1e}, K_{2i}, and K_{2e}, for cylindrical roller bearings

Bearing No.	Bearing series NU2				Bearing No.	Bearing series NU3			
	K_{1i}	K_{1e}	K_{2i}	K_{2e}		K_{1i}	K_{1e}	K_{2i}	K_{2e}
			$\times 10^{-3}$	$\times 10^{-3}$				$\times 10^{-3}$	$\times 10^{-3}$
NU205W	30.6	25.8	2.90	3.44	NU305W	24.2	19.6	3.03	3.73
NU206W	26.1	22.2	2.87	3.39	NU306W	20.5	16.8	2.89	3.52
NU207W	21.6	18.2	2.83	3.36	NU307W	17.7	14.6	2.76	3.35
NU208W	18.5	15.7	2.70	3.20	NU308W	16.1	13.4	2.76	3.32
NU209W	17.7	15.2	2.63	3.07	NU309W	14.4	11.8	2.85	3.46
NU210W	17.0	14.7	2.55	2.95	NU310W	13.1	10.8	2.79	3.37
NU211W	15.4	13.3	2.54	2.93	NU311W	11.5	9.44	2.76	3.36
NU212W	14.0	12.2	2.53	2.92	NU312W	10.8	8.91	2.76	3.34
NU213W	12.5	10.8	2.44	2.82	NU313W	10.3	8.54	2.79	3.37
NU214W	12.4	10.9	2.45	2.81	NU314W	9.35	7.78	2.68	3.22
NU215W	11.5	10.1	2.44	2.80	NU315W	8.83	7.31	2.77	3.34
NU216W	11.0	9.57	2.49	2.86	NU316W	8.43	7.05	2.68	3.20
NU217W	10.2	8.94	2.48	2.85	NU317W	8.04	6.68	2.76	3.32
NU218W	9.10	7.87	2.45	2.84	NU318W	7.45	6.22	2.68	3.21
NU219W	8.98	7.77	2.56	2.96	NU319W	7.14	5.97	2.68	3.20
NU220W	8.23	7.13	2.47	2.85	NU320W	6.61	5.52	2.66	3.19
NU221W	7.82	6.78	2.47	2.85	NU321W	6.42	5.34	2.76	3.31
NU222W	7.36	6.34	2.53	2.93	NU322W	6.06	5.04	2.78	3.34
NU224W	7.02	6.08	2.53	2.92	NU324W	5.38	4.44	2.75	3.33
NU226W	6.76	5.91	2.46	2.82	NU326W	5.07	4.21	2.75	3.32
NU228W	6.27	5.48	2.47	2.83	NU328W	4.80	3.99	2.75	3.31
NU230W	5.80	5.07	2.47	2.83	NU330W	4.61	3.85	2.79	3.34

Table 2 Constants, K_{1i}, K_{1e}, K_{2i}, and K_{2e}, for cylindrical roller bearings

Bearing No.	Bearing series NU4				Bearing No.	Bearing series NU22			
	K_{1i}	K_{1e}	K_{2i}	K_{2e}		K_{1i}	K_{1e}	K_{2i}	K_{2e}
			$\times 10^{-3}$	$\times 10^{-3}$				$\times 10^{-3}$	$\times 10^{-3}$
NU405W	19.2	15.1	3.08	3.92	NU2205W	25.4	21.4	2.40	2.85
NU406W	16.4	12.9	3.06	3.90	NU2206W	21.1	17.9	2.32	2.73
NU407W	14.6	11.7	2.99	3.74	NU2207W	17.0	14.3	2.22	2.63
NU408W	12.9	10.2	2.96	3.73	NU2208W	15.4	13.0	2.25	2.66
NU409W	12.0	9.65	2.97	3.70	NU2209W	14.7	12.6	2.18	2.55
NU410W	10.9	8.73	2.98	3.73	NU2210W	14.1	12.3	2.12	2.45
NU411W	10.3	8.37	2.87	3.54	NU2211W	13.0	11.3	2.15	2.48
NU412W	9.35	7.56	2.85	3.52	NU2212W	11.3	9.79	2.04	2.35
NU413W	8.90	7.23	2.85	3.51	NU2213W	9.93	8.62	1.94	2.24
NU414W	7.90	6.41	2.86	3.52	NU2214W	9.88	8.64	1.95	2.23
NU415W	7.34	5.92	2.84	3.52	NU2215W	9.54	8.32	2.02	2.32
NU416W	6.84	5.50	2.82	3.51	NU2216W	8.90	7.76	2.02	2.31
NU417M	6.49	5.18	2.83	3.55	NU2217W	8.22	7.17	1.99	2.28
NU418M	6.07	4.87	2.83	3.53	NU2218W	7.46	6.45	2.01	2.33
NU419M	5.76	4.69	2.73	3.36	NU2219W	7.03	6.08	2.00	2.32
NU420M	5.44	4.41	2.72	3.35	NU2220W	6.82	5.90	2.05	2.36
NU421M	5.15	4.17	2.71	3.35	NU2221M	6.44	5.58	2.03	2.34
NU422M	4.87	3.95	2.71	3.34	NU2222W	5.96	5.14	2.05	2.38
NU424M	4.37	3.54	2.72	3.37	NU2224W	5.65	4.89	2.03	2.35
NU426M	3.92	3.16	2.71	3.36	NU2226W	5.28	4.61	1.92	2.20
NU428M	3.80	3.07	2.74	3.38	NU2228W	4.82	4.22	1.90	2.18
NU430M	2.97	2.97	2.65	3.23	NU2230W	4.55	3.98	1.93	2.21

Table 3 Constants, K_{1i}, K_{1e}, K_{2i}, and K_{2e}, for cylindrical roller bearings

Bearing No.	Bearing series NU23				Bearing No.	Bearing series NN30			
	K_{1i}	K_{1e}	K_{2i}	K_{2e}		K_{1i}	K_{1e}	K_{2i}	K_{2e}
			$\times 10^{-3}$	$\times 10^{-3}$				$\times 10^{-3}$	$\times 10^{-3}$
NU2305W	19.0	15.4	2.38	2.93	NN3005	31.3	27.3	2.36	2.72
NU2306W	17.0	14.0	2.41	2.93	NN3006	28.1	24.7	2.36	2.69
NU2307W	15.6	12.9	2.43	2.96	NN3007T	24.3	21.5	2.24	2.53
NU2308W	12.9	10.7	2.22	2.67	NN3008T	23.1	20.4	2.31	2.61
NU2309W	11.9	9.79	2.36	2.86	NN3009T	20.7	18.4	2.25	2.52
NU2310W	10.6	8.76	2.26	2.73	NN3010T	20.1	18.1	2.20	2.45
NU2311W	9.53	7.83	2.29	2.78	NN3011T	17.5	15.6	2.18	2.43
NU2312W	8.85	7.31	2.26	2.74	NN3012T	16.7	15.0	2.09	2.32
NU2313W	8.32	6.90	2.26	2.72	NN3013T	15.9	14.5	2.02	2.22
NU2314W	7.50	6.24	2.15	2.58	NN3014T	14.4	13.0	2.04	2.25
NU2315W	6.98	5.78	2.19	2.64	NN3015T	14.0	12.8	2.01	2.20
NU2316W	6.66	5.58	2.11	2.53	NN3016T	12.6	11.4	1.99	2.19
NU2317W	6.21	5.17	2.14	2.57	NN3017T	12.3	11.2	1.96	2.15
NU2318W	6.11	5.10	2.20	2.63	NN3018T	11.4	10.3	1.98	2.18
NU2319W	5.65	4.73	2.12	2.53	NN3019T	11.1	10.2	1.95	2.14
NU2320W	5.40	4.51	2.18	2.60	NN3020T	10.9	10.0	1.92	2.09
NU2321M	4.80	3.99	2.06	2.48	NN3021T	9.75	8.84	2.00	2.21
NU2322M	4.48	3.73	2.05	2.47	NN3022T	9.04	8.18	2.00	2.20
NU2324M	4.00	3.31	2.05	2.48	NN3024T	8.66	7.90	1.93	2.11
NU2326M	3.62	3.00	1.96	2.37	NN3026T	7.86	7.14	1.99	2.19
NU2328M	3.43	2.86	1.97	2.36	NN3028	7.55	6.90	1.92	2.11
NU2330M	3.24	2.70	1.96	2.34	NN3030	7.08	6.47	1.92	2.10

Table 4 Constants, K_{1i}, K_{1e}, K_{2i}, and K_{2e}, for tapered roller bearings

Bearing No.	Bearing series 302				Bearing No.	Bearing series 303			
	K_{1i}	K_{1e}	K_{2i}	K_{2e}		K_{1i}	K_{1e}	K_{2i}	K_{2e}
			$\times 10^{-3}$	$\times 10^{-3}$				$\times 10^{-3}$	$\times 10^{-3}$
HR30205J	20.6	17.4	1.94	2.29	HR30305J	17.8	14.3	2.34	2.92
HR30206J	17.7	14.9	1.99	2.36	HR30306J	15.7	12.8	2.30	2.83
HR30207J	15.8	13.3	2.07	2.45	HR30307J	13.7	11.1	2.26	2.78
HR30208J	14.5	12.3	2.13	2.52	HR30308J	12.1	10.0	2.09	2.51
HR30209J	13.7	11.7	2.03	2.37	HR30309J	10.9	9.07	2.11	2.54
HR30210J	12.7	11.0	1.96	2.28	HR30310J	10.1	8.37	2.16	2.60
HR30211J	11.4	9.80	2.02	2.36	HR30311J	9.38	7.79	2.19	2.64
HR30212J	11.0	9.41	2.11	2.46	HR30312J	8.66	7.19	2.19	2.64
HR30213J	10.0	8.62	2.05	2.38	HR30313J	8.04	6.68	2.20	2.65
HR30214J	9.62	8.28	2.07	2.40	HR30314J	7.49	6.22	2.20	2.65
HR30215J	9.11	7.89	1.99	2.30	HR30315J	7.09	5.88	2.23	2.68
HR30216J	8.79	7.57	2.12	2.47	HR30316J	6.79	5.64	2.28	2.74
HR30217J	8.04	6.93	2.07	2.40	HR30317J	6.30	5.24	2.22	2.68
HR30218J	7.69	6.63	2.10	2.44	30318	6.42	5.34	2.41	2.89
HR30219J	7.27	6.26	2.11	2.45	30319	6.09	5.06	2.37	2.85
HR30220J	6.74	5.81	2.07	2.40	30320	5.84	4.86	2.43	2.92
HR30221J	6.36	5.48	2.06	2.39	30321	5.62	4.67	2.44	2.94
HR30222J	5.94	5.12	2.03	2.36	HR30322J	4.99	4.15	2.33	2.81
HR30224J	5.74	4.97	2.06	2.38	HR30324J	4.75	3.95	2.39	2.88
30226	5.83	5.07	2.23	2.57	30326	4.69	3.93	2.46	2.94
HR30228J	5.36	4.64	2.24	2.58	30328	4.47	3.75	2.50	2.98
30230	5.10	4.41	2.31	2.67	30330	4.15	3.48	2.50	2.98

Table 5 Constants, K_{1i}, K_{1e}, K_{2i}, and K_{2e}, for tapered roller bearings

Bearing No.	Bearing series 322				Bearing No.	Bearing series 323			
	K_{1i}	K_{1e}	K_{2i}	K_{2e}		K_{1i}	K_{1e}	K_{2i}	K_{2e}
			$\times 10^{-3}$	$\times 10^{-3}$				$\times 10^{-3}$	$\times 10^{-3}$
HR32205	18.5	15.6	1.72	2.04	HR32305J	15.0	12.0	1.93	2.40
HR32206J	15.7	13.2	1.76	2.08	HR32306J	12.9	10.5	1.86	2.28
HR32207J	13.3	11.2	1.73	2.05	HR32307J	11.5	9.38	1.87	2.30
HR32208J	12.8	10.8	1.88	2.22	HR32308J	10.1	8.38	1.71	2.06
HR32209J	12.0	10.3	1.79	2.09	HR32309J	9.22	7.65	1.75	2.11
HR32210J	11.7	10.0	1.80	2.08	HR32310J	8.26	6.86	1.73	2.08
HR32211J	10.4	8.90	1.83	2.14	HR32311J	7.62	6.33	1.74	2.10
HR32212J	9.43	8.08	1.80	2.10	HR32312J	7.13	5.92	1.77	2.13
HR32213J	9.64	7.40	1.82	2.13	HR32313J	6.62	5.50	1.78	2.15
HR32214J	8.58	7.39	1.84	2.14	HR32314J	6.21	5.16	1.79	2.16
HR32215J	8.28	7.18	1.81	2.09	HR32315J	5.80	4.81	1.79	2.15
HR32216J	7.70	6.63	1.86	2.15	HR32316J	5.46	4.54	1.80	2.16
HR32217J	7.38	6.36	1.90	2.21	HR32317J	5.26	4.36	1.83	2.20
HR32218J	6.56	5.65	1.80	2.09	HR32318J	5.00	4.15	1.83	2.20
HR32219J	6.14	5.29	1.78	2.07	32319	4.97	4.13	1.89	2.27
HR32220J	5.77	4.97	1.77	2.06	HR32320J	4.43	3.68	1.84	2.21
HR32221J	5.39	4.64	1.74	2.02	32321	4.36	3.62	1.88	2.27
HR32222J	5.12	4.41	1.75	2.03	HR32322J	4.03	3.35	1.87	2.25
HR32224J	4.82	4.18	1.72	1.98	HR32324J	3.75	3.11	1.87	2.25
32226	4.48	3.90	1.68	1.93	32326	3.59	3.01	1.89	2.26
HR32228J	4.02	3.48	1.67	1.93	32328	3.21	2.71	1.75	2.08
32230	4.06	3.55	1.74	1.99	32330	2.95	2.51	1.65	1.94

Table 6 Constants, K_{1i}, K_{1e}, K_{2i}, and K_{2e}, for tapered roller bearings

Bearing No.	Bearing series 303D				Bearing No.	Bearing series 320			
	K_{1i}	K_{1e}	K_{2i}	K_{2e}		K_{1i}	K_{1e}	K_{2i}	K_{2e}
			$\times 10^{-3}$	$\times 10^{-3}$				$\times 10^{-3}$	$\times 10^{-3}$
30305D	22.0	18.4	2.42	2.91	HR32005XJ	21.1	18.4	1.58	1.82
30306D	19.0	15.8	2.48	2.98	HR32006XJ	18.2	15.9	1.61	1.85
HR30307DJ	14.8	12.4	2.18	2.62	HR32007XJ	16.4	14.4	1.57	1.79
HR30308DJ	13.0	10.8	2.18	2.61	HR32008XJ	14.4	12.7	1.48	1.67
HR30309DJ	11.9	9.94	2.22	2.66	HR32009XJ	13.3	11.8	1.47	1.65
HR30310DJ	10.8	9.02	2.21	2.65	HR32010XJ	13.0	11.6	1.45	1.62
HR30311DJ	10.0	8.37	2.22	2.66	HR32011XJ	11.3	10.0	1.46	1.64
HR30312DJ	9.33	7.79	2.26	2.71	HR32012XJ	10.8	9.69	1.41	1.57
HR30313DJ	8.66	7.23	2.27	2.71	HR32013XJ	10.6	9.57	1.39	1.54
HR30314DJ	8.20	6.85	2.28	2.74	HR32014XJ	9.68	8.70	1.44	1.60
HR30315DJ	7.83	6.54	2.34	2.80	HR32015XJ	9.32	8.43	1.39	1.54
HR30316DJ	7.37	6.15	2.33	2.80	HR32016XJ	8.15	7.35	1.36	1.51
HR30317DJ	6.93	5.79	2.34	2.80	HR32017XJ	8.00	7.25	1.34	1.48
HR30318DJ	6.96	5.81	2.48	2.98	HR32018XJ	7.36	6.64	1.37	1.52
HR30319DJ	6.34	5.30	2.37	2.84	HR32019XJ	7.22	6.54	1.35	1.50
—	—	—	—	—	HR32020XJ	7.10	6.45	1.34	1.47
—	—	—	—	—	HR32021XJ	6.61	5.99	1.36	1.50
—	—	—	—	—	HR32022XJ	6.19	5.59	1.39	1.54
—	—	—	—	—	HR32024XJ	6.10	5.52	1.42	1.56
—	—	—	—	—	HR32026XJ	5.26	4.74	1.41	1.57
—	—	—	—	—	HR32028XJ	5.15	4.67	1.39	1.54
—	—	—	—	—	HR32030XJ	4.77	4.32	1.38	1.53

5.6 Rolling contact trace and load conditions

5.6.1 Ball bearing

When a rolling bearing is rotating while subjected to a load on the raceways of the inner and outer rings and on the surfaces of the rolling elements, heavy stress is generated at the place of contact. For example, when about 10% of the load (normal load) of the C_r, basic dynamic load rating, as radial load, is applied, in the case of deep groove ball bearings, its maximum surface pressure becomes about 2 000 MPa {204 kgf/mm^2} and for a roller bearing, the pressure reaches 1 000 MPa {102 kgf/mm^2}.

As bearings are used under such high contact surface pressure, the contact parts of the rolling elements and raceway may become slightly elastically deformed or wearing may progress depending on lubrication conditions. As a result of this contact trace, light reflected from the raceway surface of a used bearing looks different for the places where a load was not applied.
Parts that were subjected to load reflect light differently and the dull appearance of such parts is called a trace (rolling contact trace). Thus, an examination of the trace can provide insights into the contact and load conditions.

Trace varies depending on the bearing type and conditions. Examination of the trace sometimes allows identification of the cause: radial load only, heavy axial load, moment load, or extreme unevenness of stiffness of housing.

For the case of a deep groove ball bearing used under an inner ring rotation load, only radial load F_r is applied, under the general condition of residual clearance after mounting is $\Delta_r>0$, the load zone ψ becomes narrower than 180° (Fig. 1), traces on inner and outer rings become as shown in Fig. 2.

In addition to a radial load F_r, if an axial load F_a is simultaneously applied, the load zone ψ is widened as shown in Fig. 3. When only an axial load is applied, all rolling elements are uniformly subjected to the load, for both inner and outer rings the load zone becomes ψ=360° and the race is unevenly displaced in the axial direction.

A deviated and inclined trace may be observed on the outer ring as shown in Fig. 4, when an axial load and relative inclination of the inner ring to the outer ring are applied together to a deep groove or angular contact ball bearing used for inner ring rotation load. Or if the deflection is big, a similar trace appears.

As explained above, by comparing the actual trace with the shape of the trace forecasted from the external force considered when the bearing was designed, it is possible to tell if an abnormal axial load was applied to the bearing or if the mounting error was excessive.

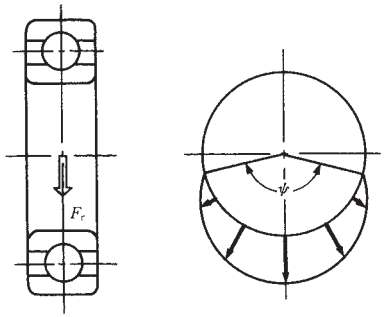

Fig. 1 Load zone under a radial load only

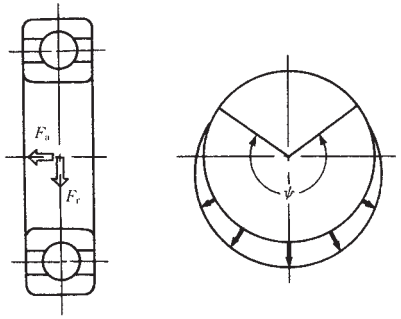

Fig. 3 Load zone for radial load + axial load

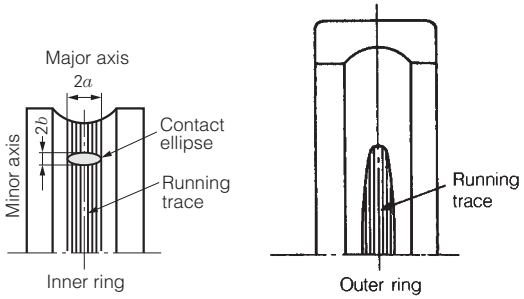

Fig. 2 Trace (rolling contact trace) on raceway surface

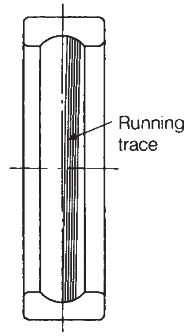

Fig. 4 Deviation and inclination of trace (rolling contact trace) on raceway surface of outer ring

5.6.2 Roller bearing

The relation between load condition and running trace of roller bearings may be described as follows. Usually, when rollers (or raceway) of a roller bearing are not crowned despite there being no relative inclination on inner ring with outer ring, then stress concentration occurs at the end parts where the rollers contact the raceway (Fig. 5 (a)). Noticeable contact appears at both ends of the trace. If the stress on the end parts is excessive, premature flaking occurs. Rollers (or raceway) can be crowned to reduce stress (Fig. 5 (b)). Even if the rollers are crowned, however, if inclination exists between the inner and outer rings, then stress at the contacting part becomes as shown in Fig. 5 (c).

Fig. 6 (a) shows an example of trace on an outer ring raceway for a radial load which is correctly applied to a cylindrical roller bearing and used for inner ring rotation. Compared with this, if there is relative inclination of inner ring to outer ring, as shown in Fig. 6 (b), the trace on raceway has shading in width direction. And the trace looks inclined at the entry and exit of the load zone.

The trace of outer ring becomes as shown in Fig. 7 (a) for double-row tapered roller bearings if only a radial load is applied while inner ring is rotating, or the trace becomes as shown in Fig. 7 (b) if only an axial load is applied.
In addition, traces are produced on both sides of the raceway (displaced by 180°) as shown in Fig. 7 (c) if a radial load is applied under the condition that there is a large relative inclination of the inner ring to the outer ring.

The trace becomes even on the right and left sides of the raceways if a radial load is applied to a spherical roller bearing having the permissible aligning angle of 1 to 2.5°. In the case of an application of an axial load, the trace appears only on one side. A trace is produced that has a difference corresponding to them and is marked on right and left load zones if combined radial and axial loads are applied.

Therefore, the trace becomes even on the left and right sides for a free-end spherical roller bearing that is mainly subjected to radial load. If the length of the trace is greatly different, it indicates that internal axial load caused by thermal expansion of shaft, etc. was not sufficiently absorbed by displacement of the bearing in the axial direction.

Besides the above, the trace on raceway is influenced often by the shaft or housing. By comparison of the bearing outside face contact or pattern of fretting against the degree of trace on raceway, it is possible to tell if there is structural failure or uneven stiffness of shaft or housing.

As explained above, observation of the trace on raceway can help to prevent bearing trouble.

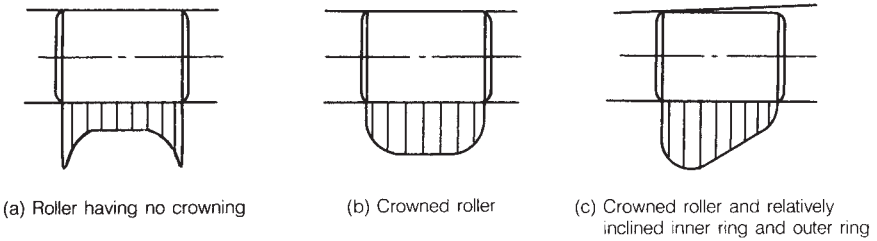

(a) Roller having no crowning (b) Crowned roller (c) Crowned roller and relatively inclined inner ring and outer ring

Fig. 5 Stress distribution of cylindrical roller

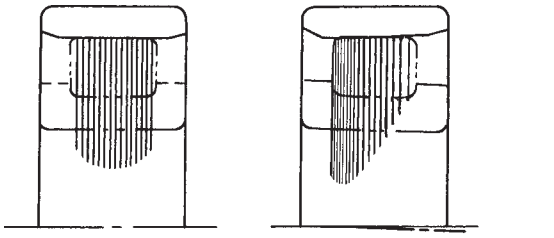

(a) Normal trace (b) When inner ring and outer ring are relatively inclined

Fig. 6 Trace (rolling contact trace) of outer ring of cylindrical roller bearing

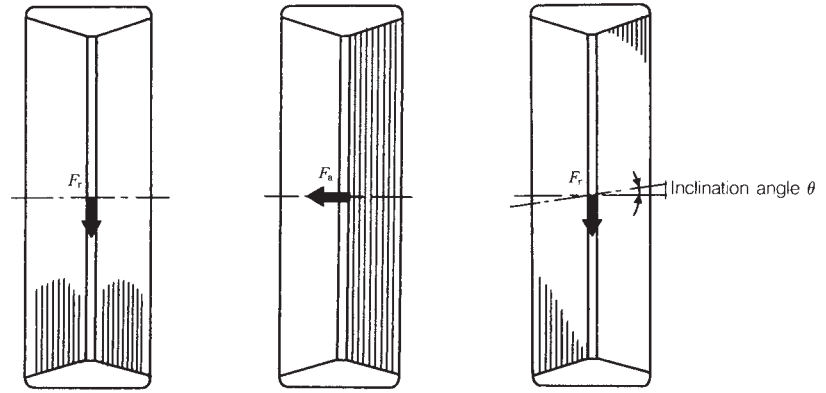

(a) When only a radial load is applied (b) When only an axial load is applied (c) When radial load is applied and inclination is large

Fig. 7 Trace (rolling contact trace) of outer ring of double row tapered roller bearing

5.7 Radial load and displacement of cylindrical roller bearings

One of the most important requirements for bearings to be used in machine-tool applications is that there be as little deflection as possible with applied loading, i.e. that the bearings have high rigidity.

Double-row cylindrical roller bearings are considered to be the most rigid types under radial loads and also best for use at high speeds. NN30K and NNU49K series are the particular radial bearings most often used in machine tool head spindles.

The amount of bearing displacement under a radial load will vary with the amount of internal clearance in the bearings. However, since machine-tool spindle cylindrical roller bearings are adjusted so the internal clearance after mounting is less than several micrometers, we can consider the internal clearance to be zero for most general calculations. The radial elastic displacement δ_r of cylindrical roller bearings can be calculated using Equation (1).

$$\left.\begin{aligned}\delta_r &= 0.000077\frac{Q_{max}^{0.9}}{L_{we}^{0.8}} \quad \text{(N)} \\ &= 0.0006\frac{Q_{max}^{0.9}}{L_{we}^{0.8}} \quad \{\text{kgf}\}\end{aligned}\right\} \text{(mm)} \cdots\cdots\cdots (1)$$

where, Q_{max}: Maximum rolling element load (N), {kgf}
L_{we}: Effective contact length of roller (mm)

If the internal clearance is zero, the relationship between maximum rolling element load Q_{max} and radial load F_r becomes:

$$Q_{max} = \frac{4.08}{iZ} F_r \quad \text{(N), \{kgf\}} \cdots\cdots\cdots (2)$$

where, i: Number of rows of rollers in a bearing (double-row bearings: i=2)
Z: Number of rollers per row
F_r: Radial load (N), {kgf}

Combining Equations (1) and (2), it follows that the relation between radial load F_r and radial displacement δ_r becomes.

$$\left.\begin{aligned}\delta_r &= K F_r^{0.9} \quad \text{(N)} \\ &= 7.8K F_r^{0.9} \quad \{\text{kgf}\}\end{aligned}\right\} \text{(mm)} \cdots\cdots\cdots (3)$$

where, $K = \dfrac{0.000146}{Z^{0.9} L_{we}^{0.8}}$

K is a constant determined by the individual double-row cylindrical roller bearing. Table 1 gives values for K for bearing series NN30. Fig. 1 shows the relation between radial load F_r and radial displacement δ_r.

Table 1 Constant K for bearing series NN30

Bearing	K	Bearing	K	Bearing	K
	$\times 10^{-6}$		$\times 10^{-6}$		$\times 10^{-6}$
NN3005	3.31	NN3016T	1.34	NN3032	0.776
NN3006T	3.04	NN3017T	1.30	NN3034	0.721
NN3007T	2.56	NN3018T	1.23	NN3036	0.681
NN3008T	2.52	NN3019T	1.19	NN3038	0.637
NN3009T	2.25	NN3020T	1.15	NN3040	0.642
NN3010T	2.16	NN3021T	1.10	NN3044	0.581
NN3011T	1.91	NN3022T	1.04	NN3048	0.544
NN3012T	1.76	NN3024T	0.966	NN3052	0.526
NN3013T	1.64	NN3026T	0.921	NN3056	0.492
NN3014T	1.53	NN3028	0.861	NN3060	0.474
NN3015T	1.47	NN3030	0.816	NN3064	0.444

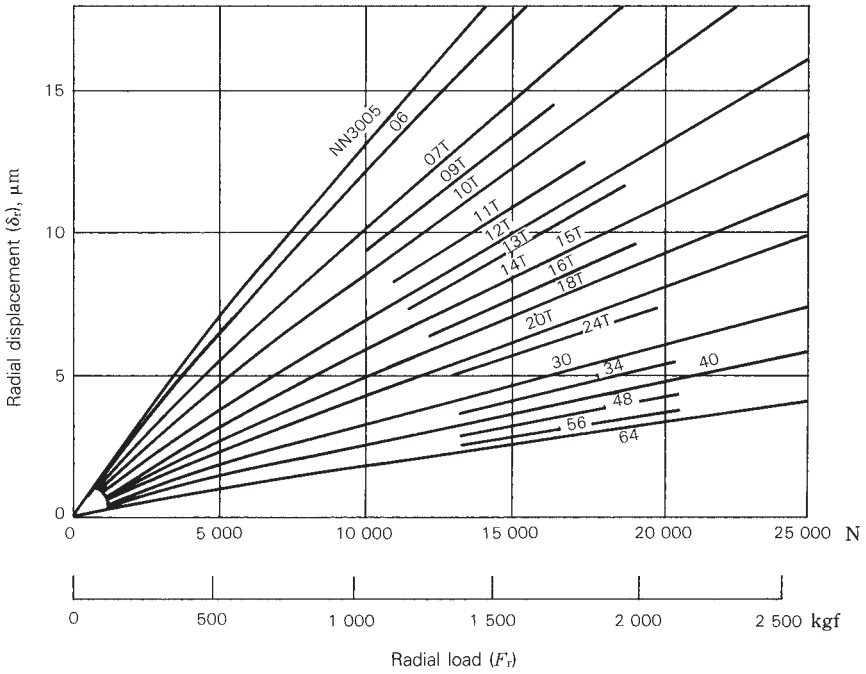

Fig. 1

5.8 Misalignment, maximum rolling-element load and moment for deep groove ball bearings

5.8.1 Misalignment angle of rings and maximum rolling-element load

There are occasions when the inner and outer rings of deep groove bearings are forced to rotate out of parallel, whether from shaft deflection or mounting error. The allowable misalignment can be determined from the relation between the inner or outer ring deflection angle θ and maximum rolling-element load Q_{max}.

For standard groove radii, the relation between θ and Q_{max} (see Fig. 1) is given by Equation (1).

$$Q_{max}=K\,D_w^{\,2}\left\{\sqrt{\left(\frac{R_i}{2m_0}\theta\right)^2+\cos^2\alpha_0}-1\right\}^{3/2}$$

(N), {kgf} ..... (1)

where, K: Constant determined by bearing material and design
Approximately for deep groove ball bearing
K=717 (N-unit)
K=72.7 {kgf-unit}

Q_{max}: Maximum rolling element load (N), {kgf}

D_w: Ball diameter (mm)

R_i: Distance between bearing center and inner ring raceway curvature center (mm)

m_0: $m_0=r_i+r_e-D_w$
r_i and r_e are inner and outer ring groove radii, respectively

θ: Inner and outer ring misalignment angle (rad)

α_0: Initial contact angle (°)

$$\cos\alpha_0=1-\frac{\Delta_r}{2m_0}$$

Δ_r: Radial clearance (mm)

Fig. 2 shows the relationship between θ and Q_{max} for a 6208 ball bearing with various radial clearances Δ_r.

When a radial load F_r equivalent to the basic static load rating C_{0r}=17 800 N {1 820 kgf} or basic dynamic load rating C_r=29 100 N {2 970 kgf} is applied on a bearing, Q_{max} becomes as follows by Equation 8 in Section 5.1.

$F_r=C_{0r}$ Q_{max}=9 915 N {1 011 kgf}
$F_r=C_r$ Q_{max}=16 167 N {1 650 kgf}

Since the allowable misalignment θ during operation will vary depending on the load, it is impossible to make an unqualified statement, but if we reasonably assume Q_{max}=2 000 N {204 kgf}, 20% of Q_{max} when $F_r=C_{0r}$, we can determine from Fig. 2 that θ will be:

Δ_r=0 θ=18′
Δ_r=0.050 mm θ=24.5′

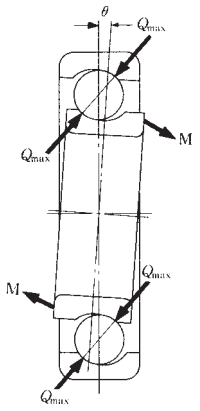

Fig. 1

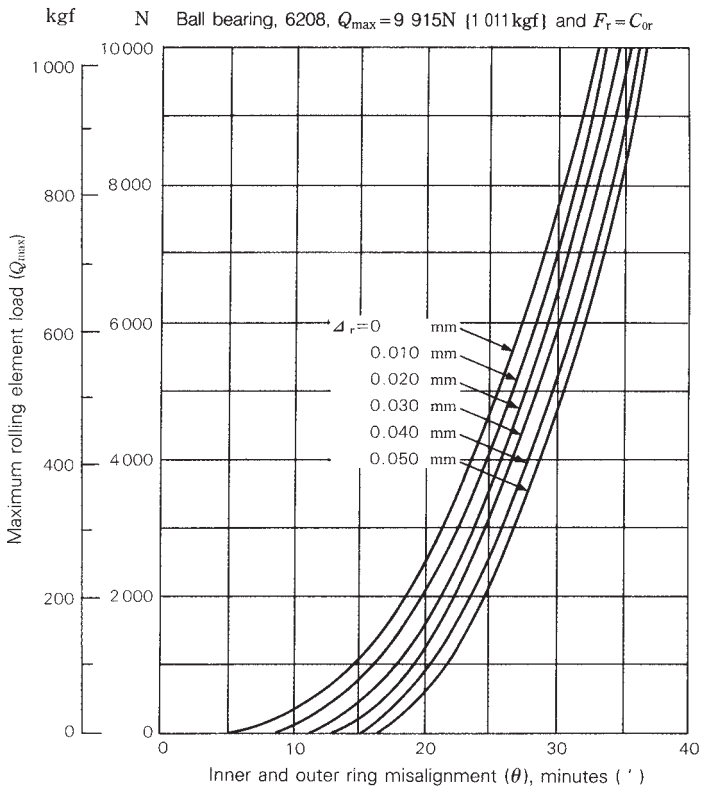

Fig. 2 Inner and outer ring misalignment and maximum rolling element load

5.8.2 Misalignment of inner and outer rings and moment

To determine the angle ψ (Fig. 3) between the positions of the ball and ball under maximum rolling-element load, for standard race way radii, Equation (2) for rolling-element load $Q(\psi)$ can be used like Equation (1) (Page 134).

$$Q(\psi)=K D_w^{2}\left\{\sqrt{\left(\frac{R_i}{m_0}\theta\right)^2\cos^2\psi+\cos^2\alpha_0}-1\right\}^{3/2}$$

(N), {kgf} ..... (2)

The moment $M(\psi)$ caused by the relative inner and outer ring misalignment from this $Q(\psi)$ is given by,

$$M(\psi)=\frac{D_{pw}}{2}\cos\psi\, Q(\psi)\sin\alpha(\psi)$$

where, D_{pw}: Ball pitch diameter (mm)
$\alpha(\psi)$, as used here, represents the local rolling element contact angle at the ψ position. It is given by,

$$\sin\alpha(\psi)=\frac{\left(\frac{R_i}{m_0}\theta\right)\cos\psi}{\sqrt{\left(\frac{R_i}{m_0}\theta\right)^2\cos^2\psi+\cos^2\alpha_0}}$$

It is better to consider that the moment M originating from bearing can be replaced with the total moment originating from individual rolling element loads. The relation between the inner and outer ring misalignment angle θ and moment M is as shown by Equation (3):

$$M=\sum_{\psi=0}^{2\pi}\frac{D_{pw}}{2}\cos\psi Q(\psi)\sin\alpha(\psi)$$

$$=\frac{KD_{pw}D_w^{2}}{2}\Sigma\frac{\left\{\sqrt{\left(\frac{R_i}{m_0}\theta\right)^2\cos^2\psi+\cos^2\alpha_0}-1\right\}^{3/2}\left(\frac{R_i}{m_0}\theta\right)\cos^2\psi}{\sqrt{\left(\frac{R_i}{m_0}\theta\right)^2\cos^2\psi+\cos^2\alpha_0}}$$

(mN·m), {kgf·mm} ..... (3)

where, K: Constant determined by bearing material and design

Figs. 4 shows the calculated results for a 6208 deep groove ball bearing with various internal clearances. The allowable moment for a 6208 bearing with a maximum rolling element load Q_{max} of 2 000 N {204 kgf}, can be estimated using Fig. 2 (Page 135):

Radial clearance Δ_r=0, θ=18′
M=60 N·m {6.2 kgf·mm}

Radial clearance Δ_r=0.050 mm θ=24.5′
M=70 N·m {7.1 kgf·mm}

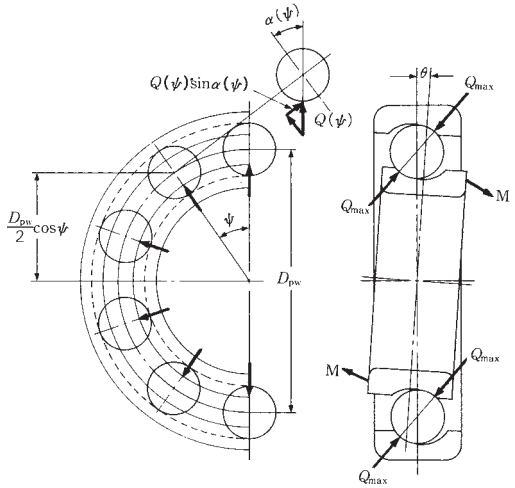

Fig. 3

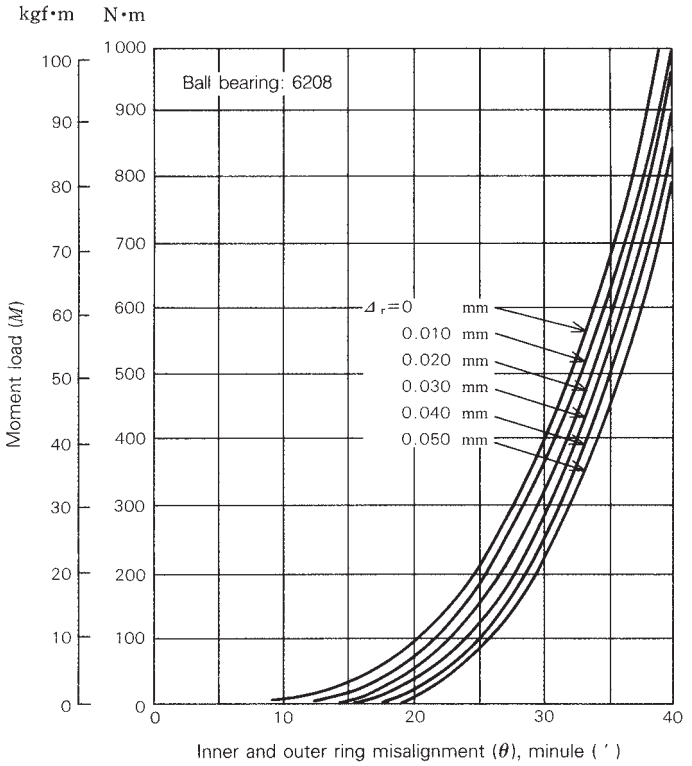

Fig. 4 Inner and outer ring misalignment and moment

5.9 Load distribution of single-direction thrust bearing due to eccentric load

When a pure axial load F_a is applied on a single-direction thrust bearing with a contact angle of α=90°, each rolling element is subjected to a uniform load Q:

$$Q=\frac{F_a}{Z}$$

where, Z: Number of rolling elements

Fig. 1 shows the distribution with any eccentric load F_a applied on a single-direction thrust bearing with a contact angle α=90°.

Based on Fig. 1, the following equations can be derived to determine the total elastic deformation δ_{max} of the rolling element under the maximum load and the elastic deformation of any other rolling element $\delta(\psi)$.

$$\delta_{max}=\delta_T+\frac{\theta D_{pw}}{2} \quad \cdots\cdots (1)$$

$$\delta(\psi)=\delta_T+\frac{\theta D_{pw}}{2}\cos\psi \quad \cdots\cdots (2)$$

From Equation (1) and (2) we obtain,

$$\delta(\psi)=\delta_{max}\left\{1-\frac{1}{2\varepsilon}(1-\cos\psi)\right\} \quad \cdots\cdots (3)$$

where,

$$\varepsilon=\frac{1}{2}\left(1+\frac{2\delta_T}{\theta D_{pw}}\right) \quad \cdots\cdots (4)$$

The load $Q(\psi)$ on any rolling element is proportional to the elastic deformation $\delta(\psi)$ of the contact surface to the t power. Thus when ψ=0, with Q_{max} representing the maximum rolling element load and δ_{max} the elastic deformation, we obtain.

$$\frac{Q(\psi)}{Q_{max}}=\left\{\frac{\delta(\psi)}{\delta_{max}}\right\}^t \quad \cdots\cdots (5)$$

t=1.5 (point contact), t=1.1 (line contact)

From Equations (3) and (5), we obtain,

$$\frac{Q(\psi)}{Q_{max}}=1-\left\{\frac{1}{2\varepsilon}(1-\cos\psi)\right\}^t \quad \cdots\cdots (6)$$

Since the eccentric load F_a acting on a bearing must be the sum of the individual rolling element loads, we obtain (Z is the number of the rolling elements),

$$F_a=\sum_{\psi=0}^{2\pi} Q(\psi)$$

$$=\sum_{\psi=0}^{2\pi} Q_{max}\left\{1-\frac{1}{2\varepsilon}(1-\cos\psi)\right\}^t$$

$$=Q_{max}\, Z\, J_A \quad \cdots\cdots (7)$$

Based on Fig. 1, the moment M acting on the shaft with ψ=90° as the axis is,

$$M=\sum_{\psi=0}^{2\pi} Q(\psi)\frac{D_{pw}}{2}\cos\psi$$

$$=\sum_{\psi=0}^{2\pi} Q_{max}\frac{D_{pw}}{2}\left\{1-\frac{1}{2\varepsilon}(1-\cos\psi)\right\}^t\cos\psi$$

$$=Q_{max}\, Z\frac{D_{pw}}{2}J_R \quad \cdots\cdots (8)$$

Values for ε and the corresponding J_A and J_R values for point contact and line contact from Equations (7) and (8) are listed in Table 1.

Sample Calculation

Find the maximum rolling element load for a 51130X single-direction thrust ball bearing (ϕ150×ϕ190×31 mm) that sustains an axial load of 10 000 N {1 020 kgf} at a position 80 mm out from the bearing center.

e=80, $D_{pw}\fallingdotseq\frac{1}{2}(150+190)=170$

$$\frac{2e}{D_{pw}}=\frac{2\times80}{170}=0.941$$

Z=32

Using Table 1, the value for J_A corresponding to $2e/D_{pw}$=0.941 is 0.157. Substituting these values into Equation (7), we obtain,

$$Q_{max}=\frac{F_a}{Z\,J_A}=\frac{10\,000}{32\times0.157}=1\,990\ (\mathrm{N})$$

$$=\frac{1\,020}{32\times0.157}=203\ \{\mathrm{kgf}\}$$

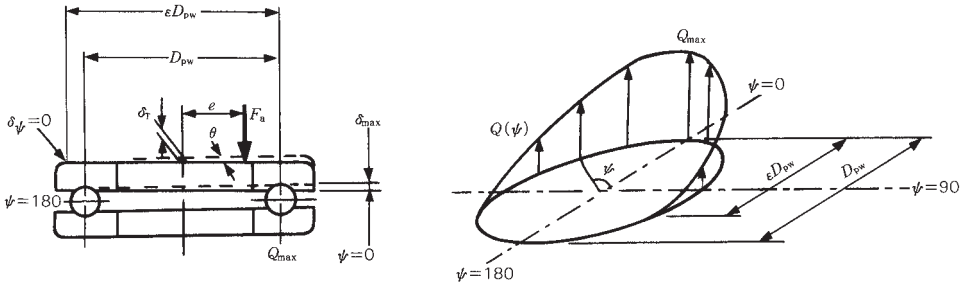

Fig. 1

Table 1 J_R and J_A values for single-direction thrust bearings

ε	Point contact			Line contact		
	$2e/D_{pw}$ $2M/D_{pw}F_a$	J_R	J_A	$2e/D_{pw}$ $2M/D_{pw}F_a$	J_R	J_A
0	1.0000	1/Z	1/Z	1.0000	1/Z	1/Z
0.1	0.9663	0.1156	0.1196	0.9613	0.1268	0.1319
0.2	0.9318	0.1590	0.1707	0.9215	0.1737	0.1885
0.3	0.8964	0.1892	0.2110	0.8805	0.2055	0.2334
0.4	0.8601	0.2117	0.2462	0.8380	0.2286	0.2728
0.5	0.8225	0.2288	0.2782	0.7939	0.2453	0.3090
0.6	0.7835	0.2416	0.3084	0.7480	0.2568	0.3433
0.7	0.7427	0.2505	0.3374	0.6999	0.2636	0.3766
0.8	0.6995	0.2559	0.3658	0.6486	0.2658	0.4098
0.9	0.6529	0.2576	0.3945	0.5920	0.2628	0.4439
1.0	0.6000	0.2546	0.4244	0.5238	0.2523	0.4817
1.25	0.4338	0.2289	0.5044	0.3598	0.2078	0.5775
1.67	0.3088	0.1871	0.6060	0.2340	0.1589	0.6790
2.5	0.1850	0.1339	0.7240	0.1372	0.1075	0.7837
5.0	0.0831	0.0711	0.8558	0.0611	0.0544	0.8909
∞	0	0	1.0000	0	0	1.0000

e: Distance between bearing center and loading point
D_{pw}: Rolling-element pitch diameter